Talanta 85 (2011) 631–637

Contents lists available at ScienceDirect

Talanta

journal homepage: www.elsevier.com/locate/talanta

A novel polybenzimidazole-modified gold electrode for the analytical determination of hydrogen peroxide

Mu-Yi Hua [a,b,*], Hsiao-Chien Chen [a,b], Rung-Ywan Tsai [c], Chao-Sung Lai [b,d]

[a] Green Technology Research Center, Department of Chemical and Materials Engineering, Chang Gung University, 259 Wen-Hwa 1st Rd., Kuei-Shan, Tao-Yuan 33302, Taiwan, ROC
[b] Biosensor Group, Biomedical Engineering Research Center, Chang Gung University, 259 Wen-Hwa 1st Rd., Kuei-Shan, Tao-Yuan 33302, Taiwan, ROC
[c] Electronics and Optoelectronics Research Laboratories, Industrial Technology Research Institute, 195, Sec. 4, Chung Hsing Rd., Hsinchu 31040, Taiwan, ROC
[d] Department of Electronic Engineering, Chang Gung University, 259 Wen-Hwa 1st Rd., Kuei-Shan, Tao-Yuan 33302, Taiwan, ROC

ARTICLE INFO

Article history:
Received 28 January 2011
Received in revised form 9 April 2011
Accepted 12 April 2011
Available online 16 April 2011

Keywords:
Sensor
Polybenzimidazole
Hydrogen peroxide
PBI *N*-oxide

ABSTRACT

The imine of polybenzimidazole (PBI) is chemically oxidized by hydrogen peroxide (H_2O_2) in the presence of acetic acid (AcOH). Fourier transform infrared (FT-IR) and X-ray photoelectron spectroscopies (XPS) showed that when the AcOH concentration remained constant, the degree of oxidation increased with increasing H_2O_2 levels. Moreover, the imine also exhibited electrochemical redox behavior. Based on these properties, a PBI-modified Au (PBI/Au) electrode was developed as an enzyme-free H_2O_2 sensor. At an applied potential of −0.5 V vs. Ag/AgCl, the current response of the PBI/Au electrode was linear with H_2O_2 concentration over a range from 0.075 to 1.5 mM, with a sensitivity of 55.0 μA mM^{-1} cm^{-2}. The probe had excellent stability, with <5% variation from its initial response current after storage at 50 °C for 10 days. Potentially interfering species such as ascorbic or uric acid had no effect on sensitivity. Sensitivity improved dramatically when multiwalled carbon nanotubes (MWCNT) were incorporated in the probe. Under optimal conditions, the detection of H_2O_2 using a MWCNT–PBI/Au electrode was linear from 1.56 μM to 2.5 mM, with a sensitivity of 928.6 μA mM^{-1} cm^{-2}. Analysis of H_2O_2 concentrations in urine samples using a MWCNT–PBI/Au electrode produced accurate real-time results comparable to those of traditional HPLC methods.

1. Introduction

Because hydrogen peroxide (H_2O_2) can induce functional and morphological disturbances and because its extreme toxicity in cells can cause cancer, its detection is important to clinical, industrial, and environmental analyses [1]. Although technologies such as titrimetry, fluorescence, and absorption spectra have been used to detect H_2O_2 [2,3], new sensors based on electrochemical technology have proven simple to use and highly sensitive for real-time detection [4,5]. Amperometric H_2O_2 sensors based on immobilized enzymes such as horseradish peroxidase (HRP), hemoglobin (Hb), or myoglobin (Mb) are widely used because of their intrinsic selectivity and sensitivity [6–8], but their performance depends on the activity of enzymes that are relatively unstable and need to be stored at 4 °C [9,10]. Thus, recent studies have aimed to measure H_2O_2 directly using enzyme-free electrodes. Although platinum nanoparticles have been used to electrocatalyze H_2O_2 directly at working potentials of 0.5–0.7 V without using enzymes [11], the selectivity at this relatively positive potential is easily compromised by interfering species such as ascorbic acid (AA) or uric acid (UA), leading to inaccurate readings [12,13]; ideally, the applied potential used to detect H_2O_2 should be negative. Metalloporphyrins used as electron-transfer mediators also possess electrocatalytic activity toward H_2O_2 [14], but their synthesis and purification are very challenging, and they must be immobilized on substrates during H_2O_2 detection. Electrodes modified with inorganic or organic–inorganic materials such as metallic nanostructures [15–17], metallic oxides [18,19], transition metals (e.g., Prussian blue) [20], or inorganic-incorporating biological complexes [21] offer stability and convenient electron transfer. However, such materials must be electrodeposited or blended with a polymer due to the poor adhesion to the electrode surface.

Polybenzimidazole (PBI) is a heterocyclic, aromatic polymer with exceptional chemical resistance, excellent mechanical

Abbreviations: AA, ascorbic acid; AcOH, acetic acid; AcOOH, peracetic acid; DMSO, dimethyl sulfoxide; FE-SEM, field-emission scanning electron microscopy; FT-IR, Fourier transform infrared spectroscopy; MWCNT, multiwalled carbon nanotubes; PBI, polybenzimidazole imine; PBINO, PBI *N*-oxide; PBI/Au, PBI-modified Au; PBS, phosphate buffer solution; UA, uric acid; XPS, X-ray photoelectron spectroscopy.

* Corresponding author at: Green Technology Research Center, Department of Chemical and Materials Engineering, Chang Gung University, 259 Wen-Hwa 1st Rd., Kuei-Shan, Tao-Yuan 33302, Taiwan, ROC. Tel.: +886 3 2118800x5289; fax: +886 3 2118668.
E-mail address: huamy@mail.cgu.edu.tw (M.-Y. Hua).

0039-9140/$ – see front matter © 2011 Elsevier B.V. All rights reserved.
doi:10.1016/j.talanta.2011.04.038

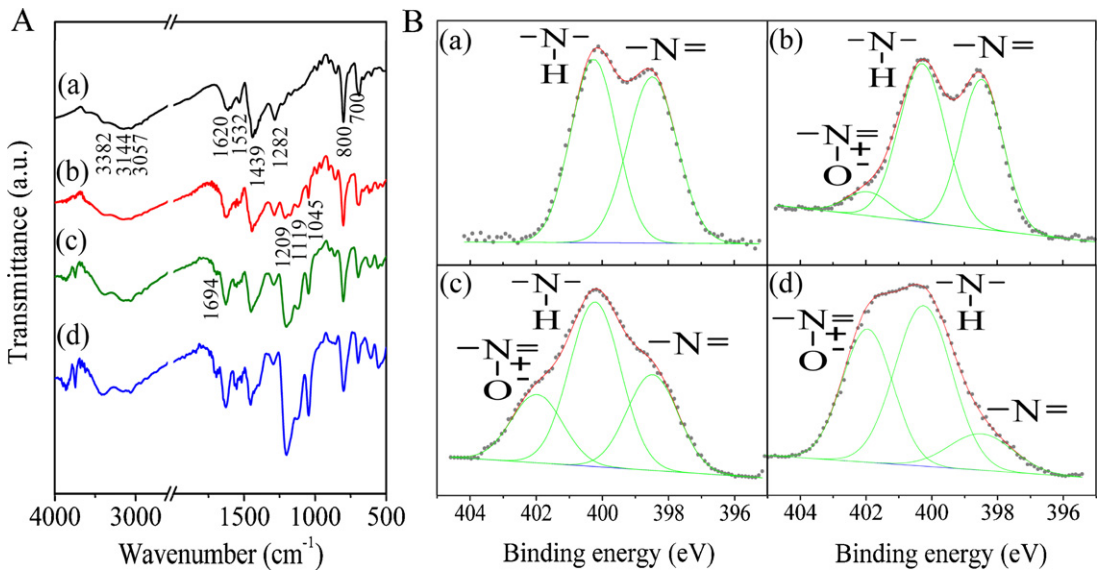

Fig. 1. (A) FT-IR spectra of (a) PBI, (b) PBINO1, (c) PBINO2, and (d) PBINO3. (B) N(1s) XPS spectra of (a) PBI, (b) PBINO1, (c) PBINO2, and (d) PBINO3.

strength, and thermal stability [22,23]. After being doped with acid, it is an excellent proton conductor and has been used in proton exchange membranes in fuel cells [24,25]. Thus far however, PBI has not been used to modify an electrode for use as an H_2O_2 sensor.

Imine structures can be oxidized by peracetic acid (AcOOH, a mixture of acetic acid (AcOH) and H_2O_2) to form *N*-oxides [26]. Furthermore, such *N*-oxides can be reduced electrochemically. In this study, the imine residue of PBI was oxidized by AcOOH to form PBI *N*-oxide (PBINO), which produced a response current during electrochemical reduction. Using this redox mechanism, a new PBI-modified Au (PBI/Au) electrode was developed to detect H_2O_2. This enzyme-free sensor exhibited superior performance, including a rapid response time, excellent stability, and good selectivity. Moreover, modifying the electrode to incorporate multiwalled carbon nanotubes (MWCNTs) enhanced the sensor's performance even further.

2. Experimental

2.1. Chemicals and reagents

Isophthaloyl dichloride (IPD, 98%) was purchased from Acros, 3,3′-diaminobenzidine tetrahydrochloride hydrate (DBT, >97%) was from Sigma–Aldrich, polyphosphoric acid and H_2O_2 (30%) were from Showa, dimethyl sulfoxide (DMSO) was from Tedia, sodium hydride was from Fluka, AcOH (99.8%) was from Scharlau, and MWCNT (S type, 10–20 nm, >95%) were from the Desunnano Co. Ltd. Deionized (DI) water saturated with nitrogen was used in all experiments.

2.2. Preparation of PBI and PBINO

PBI was synthesized by the condensation of 3,3′-diaminobenzidine tetrahydrochloride hydrate and isophthaloyl dichloride in polyphosphoric acid [27]. AcOOH solutions of 0.046, 0.091, and 0.137 M were prepared by mixing 2 M of AcOH (0.2 mmol) with 0.5 (0.1 mmol), 1.0 (0.2 mmol) and 2.0 M (0.4 mmol) of H_2O_2, respectively. PBI (0.2 mmol) was dissolved in 10 mL of DMSO and added to the AcOOH solutions. The reactions were incubated in a 43-kHz ultrasonic bath at 40 °C for 0.5 h in a dark room. After filtration, purification, and vacuum-drying at 50 °C for 24 h, precipitates of PBINO1, PBINO2 and PBINO3 (prepared from solutions with molar ratios of PBI:H_2O_2:AcOH of 1:0.5:1, 1:1:1 and 1:2:1, respectively) were obtained.

2.3. Preparation of the PBI/Au electrode

PBI (0.23 g) was dissolved in 50 mL of DMSO and concentrated to 10 mL. Two microliters of the solution were dropped onto a Au disk electrode (0.196 cm^2) and dried in a vacuum aspirator at 50 °C for 5 h.

2.4. Preparation of the MWCNT–PBI/Au electrode

To investigate the effect of the ratio (by weight) of MWCNT to PBI, samples with identical total solids content (4 μg μL^{-1}) but different weight ratios were prepared by dissolving 60 mg of PBI in 10 mL of DMSO; 20 mg of MWCNT were dispersed in 5 mL of DMSO. Forty microliters of the PBI solution were mixed with 10–320 μL of the MWCNT solution and 20 μL of DMSO were added to each solution. The currents of MWCNT–PBI/Au electrodes prepared using solutions with these different weight ratios were measured in response to 1 mM H_2O_2 in 0.2 M PBS (pH 6.4).

To determine the effect of the thickness of the composite film on the electrode surface, various volumes of a solution using the optimal weight ratio (as determined above) were dropped onto a 0.196 cm^2 Au disk electrode and dried in a vacuum aspirator at 50 °C for 5 h. The electrodes were then used to detect H_2O_2 in 0.2 M phosphate buffer solution (PBS, pH 6.4) to determine the optimal composite thickness.

2.5. Equipment and measurements

Fourier transform infrared (FT-IR) spectra were obtained with a Bruker-Tensor 27 spectrometer at a spectral resolution of 8 cm^{-1}. X-ray photoelectron spectroscopy (XPS) measurements were performed with a VG Scientific ESCALAB 250 system. Field-emission scanning electron microscopy (FE-SEM) was performed with a Hitachi S-5000 system. Electrochemical measurements were performed on a CHI 660A electrochemical workstation (CH Instruments, USA) with a three-electrode system consisting of the PBI/Au electrode, a bare Au electrode, and an Ag/AgCl electrode as the working, counter, and reference electrodes, respectively. All electrochemical measurements were performed in 40 mL of 0.2 M PBS at 25 °C and an initial pH value of 7.0. Solutions with pH values of

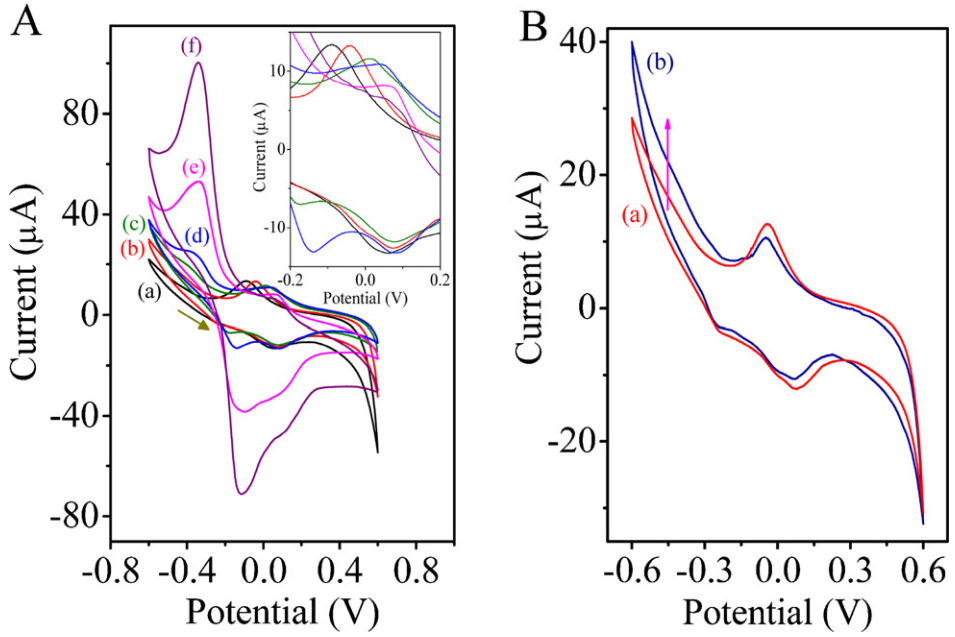

Fig. 2. (A) Cyclic voltammograms of PBI/Au electrode in 0.2 M PBS at pH values of (a) 7.0, (b) 6.4, (c) 5.2, (d) 4.6, (e) 4.1, and (f) 3.7. (B) Cyclic voltammograms of PBI/Au electrode in 0.2 M PBS at pH 6.4 in the (a) absence and (b) presence of 1 mM H_2O_2.

6.4, 5.2, 4.6, 3.7, and 3.1 were prepared by adding 0.1, 0.3, 0.5, 1, and 2 mL AcOH (99.8%) in 0.2 M PBS, respectively.

3. Results and discussion

3.1. Characterization of PBI and PBINO

The characteristic peaks of PBI as measured by FT-IR spectroscopy included the stretching vibrations (ν) of N–H (ν_{N-H}) at 3382 cm^{-1}, $\nu_{C=N/C=C}$ at 1620 cm^{-1}, in-plane deformation of the benzimidazole at 1532 and 1439 cm^{-1}, the breathing mode of the imidazole ring at 1288 cm^{-1} and the heterocyclic ring vibrations at 800 and 700 cm^{-1} (Fig. 1A) [27]. After reacting with a H_2O_2:AcOH molar ratio of 0.5:1, three additional peaks caused by the resonance structure of PBINO1 appeared at 1209 ($\nu_{N^+-O^-}$), 1119, and 1060 cm^{-1} (benzene ring in-plane C–H bending), and one new peak appeared at 1694 cm^{-1} ($\nu_{C=N^+}$) (Fig. 1A) [28]. Furthermore, the intensity of these peaks increased progressively as the molar ratio of H_2O_2:AcOH increased (Fig. 1A). This correlates with previous results showing the formation of pyridine *N*-oxide by addition of pyridine to AcOOH [26].

The N(1s) XPS spectrum of PBI can be deconvoluted into two peaks, namely imine at 398.4 eV and amine at 400.2 eV, with an area ratio for the two peaks of 1 (Fig. 1B) [29]. However, after reacting with AcOOH, the N(1s) spectrum of PBINO1 deconvoluted into three peaks: In addition to the previous two peaks, a new characteristic peak appeared at 402.0 eV, indicating the formation of *N*-oxide (Fig. 1B) [30]. The ratio of the peak areas (from lowest to highest binding energy) was 43.3:49.4:7.3, corresponding to a N_{imine}:N_{amine}:*N*-oxide ratio of 0.86:1:0.1. Thus, ~14% of the reactive sites of the imine of PBI were oxidized by AcOOH. As the molar ratios of H_2O_2:AcOH increased in PBINO2 and PBINO3, the magnitude of the 402.0 eV peak likewise increased to 41.8% and 74.6%, respectively.

3.2. Electrochemical behavior of the PBI/Au electrode

The electrochemical behavior of PBI was investigated by cyclic voltammetry at a scan rate (() of 0.05 V s^{-1} in PBS in the presence and absence of AcOH. At pH 7.0 in the absence of AcOH, the PBI/Au electrode showed a single pair of well-defined redox peaks with anodic (E_{pa}, 0.05 V) and cathodic (E_{pc}, −0.09 V) peaks between −0.6 and 0.6 V (Fig. 2A), attributed to the electroactive imine. The redox peak potentials produced by the imine structure were consistent with those seen for polyaniline [31]. As the pH decreased, the formal potential (i.e., the average of E_{pa} and E_{pc}; $E^{0'}$) of PBI shifted positively (Table 1). According to the equation $E_{Ag|AgCl|Cl^-} = E^0_{Ag|AgCl|Cl^-} - [(RT)/F] \ln a_{Cl^-}$ (where R is the universal gas constant, T is the absolute temperature, a is the chemical activity for the relevant species, and F is the Faraday constant), the standard potential for the reference electrode (Ag/AgCl) should shift positively because of the lower chemical activity (a) in the acidic solution. Decreasing the pH resulted in the formal potential of PBI shifting in the same direction. Furthermore, new redox peaks appeared in the presence of AcOH and became even more pronounced as the pH decreased. PBI was easily protonated in acidic solutions, forming $-\overset{+}{\underset{H}{N}}=$ structures [24,25]; the new redox peaks occurring at negative potentials were attributed to partial conversion of the imine to $-\overset{+}{\underset{H}{N}}=$ and corresponded with reductions in the area of the initial redox peak (as seen at pH 7.0). Using the formula $Q = nFA\Gamma$ (where Q is the charge from the anodic peak, n is the number of transferred electrons, and A is the surface area of the electrode), the surface concentration (Γ) of the original electroactive imine was estimated to be 5.73×10^{-10} mol cm^{-2} at pH 7.0; this decreased with increasing AcOH concentrations (Table 1), i.e., more imine sites were occupied by protons.

Table 1
Formal potentials ($E^{0'}$) and surface concentrations (Γ) of imine at various pH values.

pH	$E^{0'}$ (V)	Γ (10^{-10} mol cm^{-2})
7.0	−0.021	5.73
6.4	0.012	4.73
5.2	0.035	3.45
4.6	0.063	2.72
4.1	0.084	1.80
3.7	0.092	1.48

AcOOH formation:

$$H_2O_2 + AcOH \rightarrow AcOOH + H_2O$$

Chemical oxidation of PBI by AcOOH:

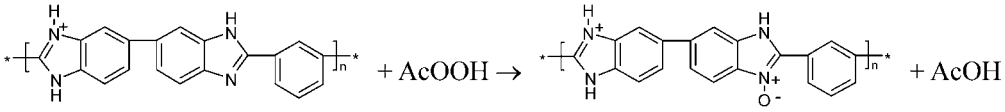

Electrochemical reduction of PBINO:

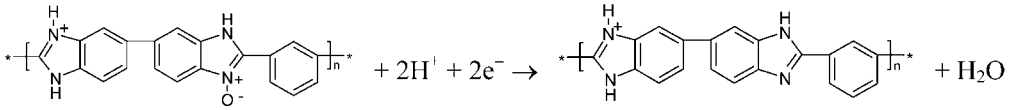

Fig. 3. Scheme of the chemical oxidation and electrochemical reduction of PBI/Au electrode in the presence of H_2O_2.

The PBI/Au electrode prepared by drop-coating had a uniformly smooth surface. Despite this planar conformation, the value of Γ (i.e., the quantity of electroactive imine that could be oxidized by AcOOH) was still higher than some enzymatic electrodes [32,33]. For enzymatic electrodes, the quantity and activity of the enzyme are the main factors influencing the surface reactivity of electroactive species. However, the amount of enzyme that can be applied to an electrode can be limited sterically by the size and/or conformation of the enzymes themselves. In contrast, the PBI/Au electrode had a higher intrinsic concentration of electroactive sites because each repeating unit along the length of the polymer chain had two reactive imines.

At pH 6.4, addition of 1 mM H_2O_2 caused a dramatic increase in the reduction current (from −0.3 to −0.6 V) and a decrease in the oxidation current. We hypothesize that the PBI was oxidized chemically by AcOOH and that the subsequent electrochemical reduction altered the response current. This is similar to results seen in enzyme-based (or some enzyme-free) H_2O_2 sensors where the probes are oxidized chemically by H_2O_2 and then reduced electrochemically to their native states [34]. Fig. 3 outlines the mechanism underlying the function of the PBI/Au electrode at reductive potentials. The redox process depends on the intrinsic properties of the PBI, which has very good stability and does not change with time because the PBI is not consumed or destroyed during the process.

3.3. An H_2O_2 sensor based on the PBI/Au electrode

To determine the conditions required for complete electrochemical reduction, current/time plots were generated at a constant applied potential of −0.5 V (i.e. lower than the first reduction peak) by successive addition of H_2O_2 to solutions with different pH values. At pH 7.0, there was no response when H_2O_2 was added, indicating that the PBI cannot be oxidized by H_2O_2 alone. In the presence of AcOH, the current response increased as H_2O_2 concentrations increased and decreased as pH values decreased (Fig. 4). The corresponding calibration curves (Fig. 4, inset) measured the performance at various pH values (Table 2). The response time at pH 6.4 was the longest, presumably because of the slow rate of AcOOH formation at the lowest AcOH concentration, but the sensitivity was highest (55.0 μA mM^{-1} cm^{-2}). This suggests that sensitivity is dominated by the surface concentration of electroactive imines that can be oxidized by AcOOH. At higher AcOH concentrations, more imine sites are occupied by protons, thus lowering the electroactivity.

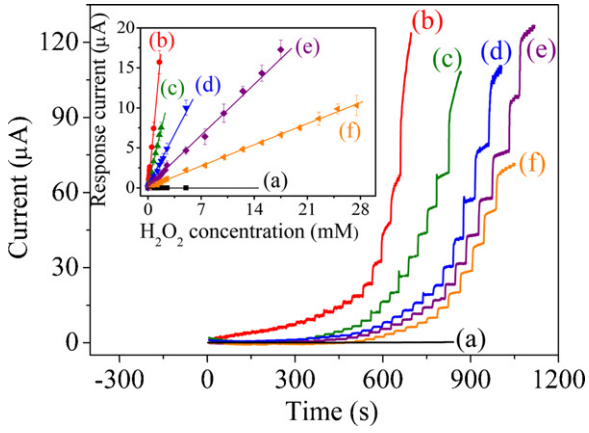

Fig. 4. Current–time responses of the PBI/Au electrode upon successive addition of H_2O_2 in 0.2 M PBS at (a) pH 7.0, (b) pH 6.4, (c) pH 5.2, (d) pH 4.6, (e) pH 4.1, and (f) pH 3.7. Inset: Plots of corresponding response currents vs. H_2O_2 concentrations.

The effects of pH on the behavior of the PBI/Au electrode provide important information. First, the process of H_2O_2 detection requires AcOH to induce chemical oxidation. Second, there was no current response in PBS at pH 7.0, meaning that no H_2O_2 reduction occurred. Furthermore, no bubbling occurred during the detection process, indicating that oxygen was not generated. This differs from some other enzyme-free H_2O_2 sensors that detect oxygen production during H_2O_2 reduction [15]. In contrast, the probe described here detects H_2O_2 via a different mechanism (i.e., the one proposed in Fig. 3).

Table 2
Effect of pH on the characteristics of the PBI/Au-based H_2O_2 sensor.

pH	Response time (s)	Sensitivity (μA mM^{-1} cm^{-2})	Detection range (mM)	R^a
7.0	–	–	–	–
6.4	7.8	55.00	0.075–1.5	0.996
5.2	7.3	21.93	0.05–1.75	0.994
4.6	6.3	10.31	0.0125–5	0.999
4.1	4.7	5.13	0.075–17.5	0.994
3.7	4.0	1.92	0.225–27.5	0.998

[a] Correlation coefficient of linear regression for response current vs. H_2O_2 concentration.

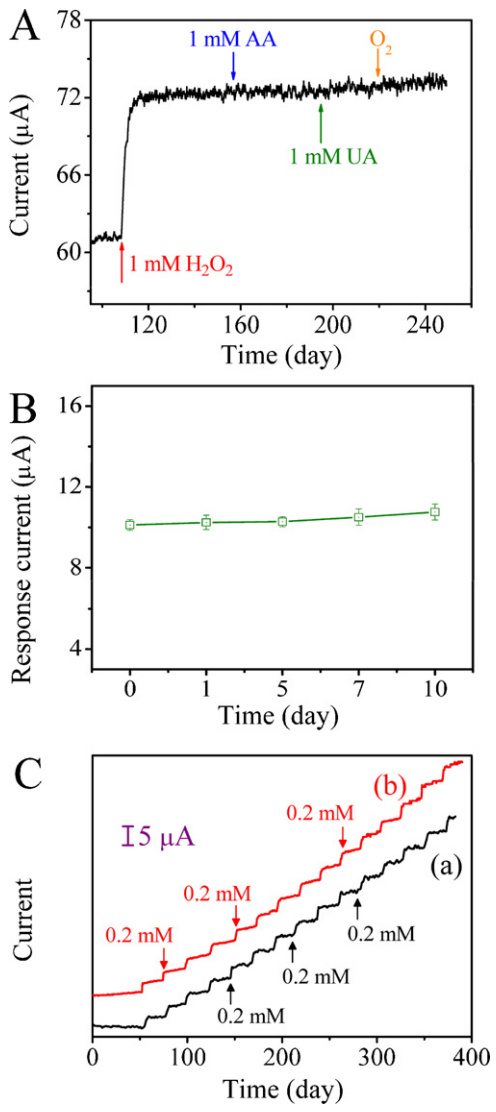

Fig. 5. (A) Effects of interfering species on the response currents of the H_2O_2 sensor based on PBI/Au electrode in 0.2 M PBS at pH 6.4. (B) The variation of response currents (1 mM H_2O_2) of the PBI/Au electrode after heat treatment at 50 °C within 10 days (pH 6.4). (C) Current–time plots of PBI/Au electrode in 0.2 M PBS at pH 6.4 with 15 sequential additions of 0.2 mM H_2O_2. (a) and (b) are the PBI/Au electrodes before and after heat-treatment at 50 °C for 10 days, respectively.

3.4. Selectivity, stability, and reproducibility of the PBI/Au electrode

The potentials required to oxidize ascorbic acid (AA) and uric acid (UA) directly are 0.25 and 0.54 V [12,34]. Thus, the ability to detect H_2O_2 at negative potentials is important because it avoids the influence of such potentially interfering substances. At the lower working potential of −0.5 V, neither AA nor UA (1 mM) interfered with the response of the PBI/Au electrode to 1 mM H_2O_2 (Fig. 5A). Injecting 40 μL of oxygen-saturated PBS also produced almost no observable variation in the response current, indicating that the sensor is highly selective.

Enzyme-modified sensors often must be stored at 4 °C to retain their activity [9,10]. Accordingly, the long-term stability of the PBI/Au electrode was investigated. After 10 days of storage at 50 °C, the response current to 1 mM H_2O_2 was altered from its initial response by <5% (Fig. 5B). Furthermore, even after 15 successive additions of 0.2 mM H_2O_2 to the heat-stored sensors, the probes displayed highly stable, detectable and repeatable currents similar to initial values (Fig. 5C); this was attributed to the intrinsic thermal stability of PBI. Finally, five successive measurements of 0.5 mM H_2O_2 resulted in a relative standard deviation of 3.9%, indicating that the sensor had good reproducibility.

3.5. A H_2O_2 sensor based on the MWCNT–PBI/Au electrode

Although the PBI/Au electrode provides a feasible and accurate means to detect H_2O_2, the highest level of sensitivity achieved was only 55.0 μA mM^{-1} cm^{-2} (Table 2). To improve the sensor's characteristics, MWCNT – which produce a highly reactive surface with good electrical conductivity – were incorporated with the PBI to produce a MWCNT–PBI/Au electrode. Two factors – weight ratio and thickness (as defined by the volume of MWCNT–PBI solution) – affect the sensitivity of MWCNT–PBI/Au electrode for the detection of H_2O_2. When the composite thickness was held constant, the amperometric response to 1 mM H_2O_2 increased gradually as the ratio (by weight) of MWCNT to PBI increased from 0.17 to 1.33, and then decreased beyond that point (Fig. 6A). FE-SEM showed that the surface area of the electrode also increased as the MWCNT/PBI weight ratio increased (Fig. 6C). When the ratio was 0.17, most MWCNT were embedded in the PBI matrix film, resulting in a relatively lower response. As the ratio increased to 0.67 and the three-dimensional surface provided more reactive surfaces (Fig. 6C), the response increased to 77.2 μA mM^{-1}. The optimal ratio (i.e., producing the highest response; 115 μA mM^{-1}) was 1.33, which produced a surface morphology for which most of the MWCNT surface was exposed (Fig. 6C). Thus, individual MWCNT can be coated with PBI, greatly enhancing PBI's reactive surface area.

The thickness of the composite on the Au electrode (which is dependent on the total solids content) also affected the sensitivity (Fig. 6B). Adding 4 μL of solution to the Au electrode produced the best response; volumes less than 4 μL might not be sufficient to cover the gold surface completely. In contrast, application of excessive amounts of solution might form a thicker layer that could restrict H_2O_2 diffusion, increasing the resistance. Thus, the optimal conditions for preparing an electrode to detect H_2O_2 in 0.2 M PBS (pH 6.4) were 4 μL of solution with a MWCNT/PBI weight ratio of 1.33.

A MWCNT–PBI/Au electrode thus prepared was tested in PBS at pH 6.4 (Fig. 7A). As the H_2O_2 concentration increased progressively, the reduction current increased immediately, reaching 95% of its steady state within 2.7 s. This was faster than the reaction time for the PBI/Au electrode (7.8 s; Table 2). Presumably, the H_2O_2 diffuses freely through the porous surface; this is consistent with other reports in the literature for porous electrodes [35]. The MWCNT–PBI/Au electrode was sensitive toward H_2O_2 in a linear range from 1.56 μM to 2.5 mM (Fig. 7B). The sensitivity was 928.6 μA mM^{-1} cm^{-2}, which was 16.9 times of that of the PBI/Au electrode (Table 2). The detection limit (0.98 μM) was estimated from the response current of a blank solution plus three times its standard deviation (i.e., 0.178 μA), divided by its linear slope (182 μA mM^{-1}). Overall, the performance of the MWCNT–PBI/Au sensor was comparable to those of other electrodes modified with MWCNT (Table 3). However, such enzyme-based sensors are limited by the number of active sites on each, possibly by steric hindrance when the enzymes are immobilized [9,36,37], whereas enzyme-free sensors that incorporate metal particles such as Au or Ag have reactive sites that are only partially (and sparsely) dispersed on MWCNT surfaces [38,39]. In contrast, there are two reactive imine sites for each repeating unit along the polymer chain in the MWCNT–PBI/Au electrode. Moreover, the PBI coats the MWCNT completely. The MWCNT–PBI/Au electrode thus offers a very rapid detection time and high sensitivity over a measurable linear range, as well as good long-term environmental stability.

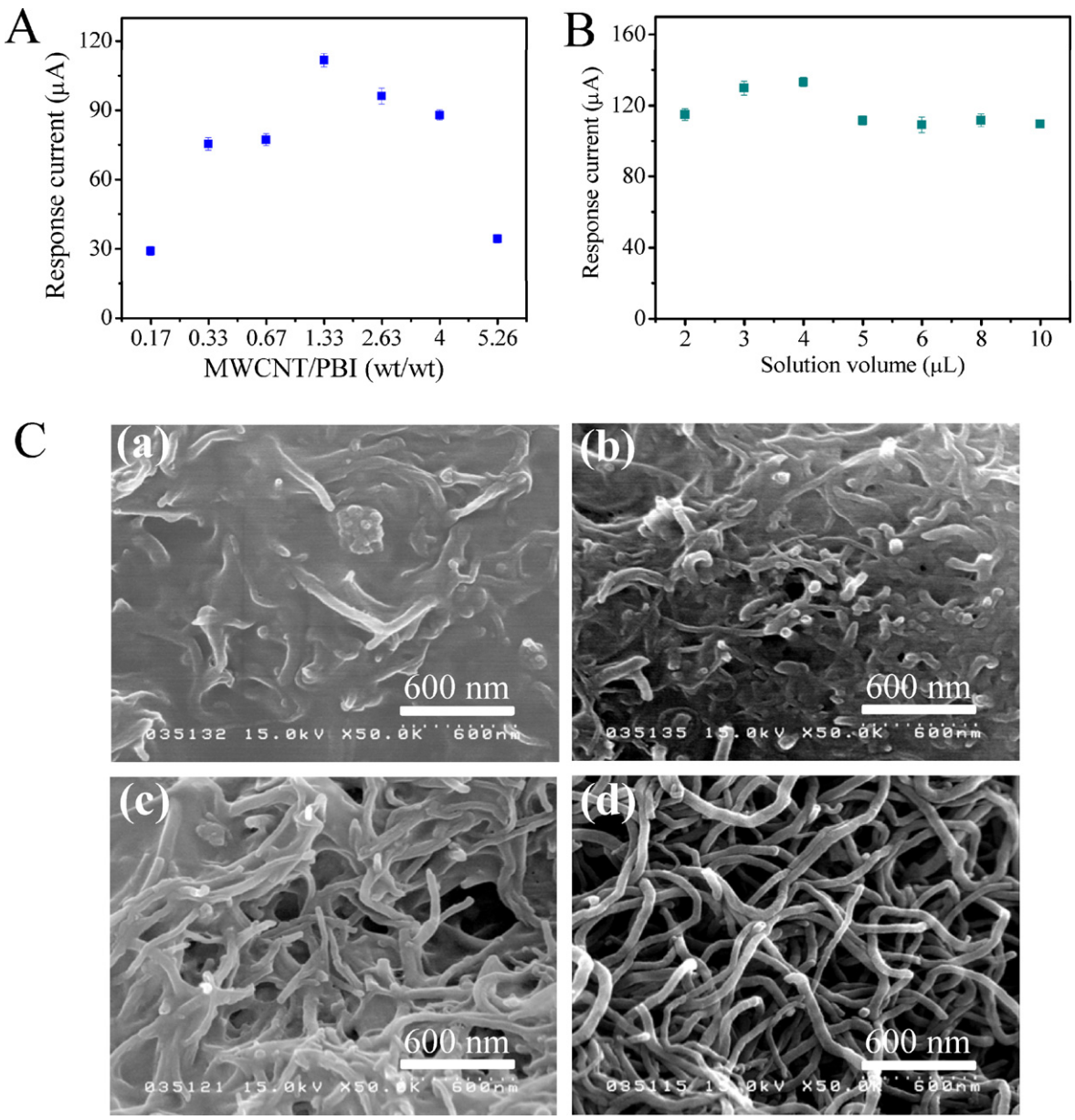

Fig. 6. Effects of (A) MWCNT/PBI weight ratios and (B) volumes of MWCNTs–PBI solutions on the response currents of MWCNTs–PBI/Au electrodes to 1 mM H_2O_2 in 0.2 M PBS at pH 6.4. (C) FE-SEM images of MWCNTs–PBI/Au electrodes with MWCNT/PBI weight ratios of (a) 0.17, (b) 0.67, and (c) 1.33. (d) Pure MWCNT.

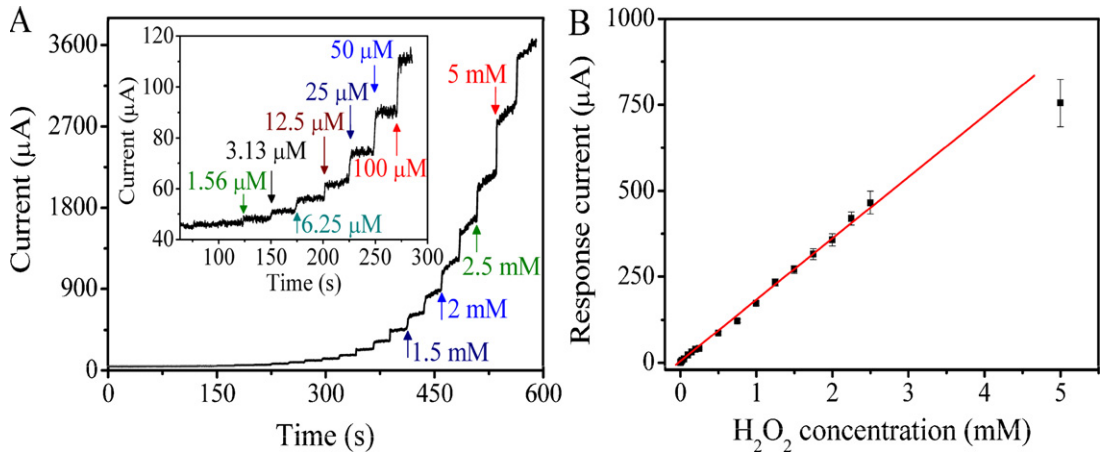

Fig. 7. (A) Current–time plot of the MWCNTs-PBI/Au electrode in 0.2 M PBS at pH 6.4 with the addition of different concentrations of H_2O_2. Inset: Response at low concentrations of H_2O_2. (B) Linear dependence of response currents vs. H_2O_2 concentrations ($n = 5$).

Table 3
Effect of sensor composition on sensor characteristics.

Electrode modification [a]	Detection range	Sensitivity ($\mu A\,mM^{-1}\,cm^{-2}$)	Response time (s)	Ref.
HRP/TTF-TCNQ/MWCNT/Au	5 μM–1.05 mM	383.0	6.0	[9]
Hb/GNP/Hb/MWCNT/GC	0.21 μM–3 mM	116.2	5.0	[37]
Hb/SA–MWCNT/GC	40 μM–0.2 mM	224.6	10.0	[36]
MWCNT–GNP–PFIL/GC	0.5 mM–18 mM	15.6	5.0	[38]
MWCNT/Ag/Au	50 μM–17 mM	20.1	5.0	[39]
MWCNT–PBI/Au	1.56 μM–2.5 mM	928.6	2.7	Present study

[a] Abbreviations: GC: glassy carbon; GNP: gold nanoparticles; Hb: hemoglobin; HRP: horseradish peroxidase; MWCNT: multiwalled carbon nanotubes; PFIL: polyethylenimine-functionalized ionic liquid; SA: sodium alginate; TTF-TCNQ: tetrathiafulvalene-tetracyanoquinodimethane.

Table 4
Comparison between the MWCNT–PBI/Au electrode and HPLC for H_2O_2 analysis.

Sample #	mM H_2O_2 detected by:	
	MWCNT–PBI/Au	HPLC
1	0.164 ± 0.008	0.150 ± 0.004
2	0.179 ± 0.008	0.162 ± 0.004
3	0.112 ± 0.006	0.099 ± 0.002
4	0.106 ± 0.006	0.095 ± 0.003

3.6. Sample analysis using the MWCNT–PBI/Au electrode

H_2O_2 is the product of oxidative stress and metabolism. To assess the utility of the proposed sensor for clinical analysis, urine samples were collected from individuals. The H_2O_2 concentrations detected in the samples by the MWCNT–PBI/Au electrode ranged from 0.11 to 0.18 mM (Table 4), comparable (albeit all slightly higher) to values obtained using a classical HPLC method of detection. However, because the anti-interference test suggested that the modified electrode was highly selective, the slight difference was attributed to some other component that might also oxidize PBI. Indeed, if the detection mechanism proposed here is accurate, PBI might also detect peroxy acids formed by other means, which might account for the consistently higher results obtained by the probe than by HPLC. Various organic acids (e.g., pyruvate, lactate, isocitrate, etc.) in human urine can also form peroxy acids in the presence of H_2O_2, which might reduce its initial concentration. However, HPLC measurements using a triphenyl phosphate probe did not identify these substances, suggesting that the sensor based on MWCNT–PBI/Au electrode might indeed provide a more sensitive and accurate means of measuring H_2O_2 concentrations in the human body.

4. Conclusions

The formation of AcOOH by AcOH after the addition of H_2O_2 oxidizes PBI and leads to an increase in response current during electrochemical reduction. This mechanism forms the basis for an enzyme-free PBI/Au electrode to detect H_2O_2 in the presence of AcOH; the sensor characteristics are tunable by adjusting the AcOH concentration. The probe is highly selective for H_2O_2 and is not influenced by interfering substances. The intrinsic properties of PBI make the electrode more stable than enzymatic sensors. Incorporating a suitable amount of MWCNT enhance all the characteristics of the sensors, presumably as a result of the increased reactive surface area and good conductivity. The detection mechanism described here also establishes a general model for H_2O_2 sensors based on polymers with imine structures that can be oxidized to form *N*-oxide and reverted to their original form by electrochemical reduction.

Acknowledgments

We thank the National Science Council and Ministry of Economic Affairs of the Republic of China, and Chang Gung University for financial aid: NSC 100-3113-E-182-001-CC2, NSC 99-2221-E-182-068, NSC 98-3114-E-182-001-CC2, A356AE1120, and CGURPD280091.

References

[1] M.C.Y. Chang, A. Pralle, E.Y. Isacoff, C.J. Chang, J. Am. Chem. Soc. 126 (2004) 15392–15393.
[2] H. Wang, S.M. Park, Anal. Chem. 79 (2007) 240–245.
[3] Z.H. Li, D.H. Li, K. Oshita, S. Motomizu, Talanta 82 (2010) 1225–1229.
[4] Y. Luo, H. Liu, Q. Rui, Y. Tian, Anal. Chem. 81 (2009) 3035–3041.
[5] X. Li, Y. Liu, A. Zhu, Y. Luo, Z. Deng, Y. Tian, Anal. Chem. 82 (2010) 6512–6518.
[6] Y. Xiao, H.X. Ju, H.Y. Chen, Anal. Biochem. 278 (2000) 22–28.
[7] A. Liu, M. Wei, I. Honma, H. Zhou, Anal. Chem. 77 (2005) 8068–8074.
[8] Z. Dai, X. Xu, H. Ju, Anal. Biochem. 332 (2004) 23–31.
[9] Z. Cao, X. Jiang, Q. Xie, S. Yao, Biosens. Bioelectron. 24 (2008) 222–227.
[10] A.K.M. Kafi, G. Wu, A. Chen, Biosens. Bioelectron. 24 (2008) 566–571.
[11] P. Karam, L.I. Halaoui, Anal. Chem. 80 (2008) 5441–5448.
[12] Y.S. Chen, J.H. Huang, C.C. Chuang, Carbon 47 (2009) 3106–3112.
[13] Y. Lin, F. Lu, Y. Tu, Z. Ren, Nano Lett. 4 (2004) 191–195.
[14] M. Hamer, R.R. Carballo, I.N. Rezzano, Electroanalysis 21 (2009) 2133–2138.
[15] W. Zhao, H. Wang, X. Qin, X. Wang, Z. Zhao, Z. Miao, L. Chen, M. Shan, Y. Fang, Q. Chen, Talanta 80 (2009) 1029–1033.
[16] S. Wang, L. Lu, M. Yang, Y. Lei, G. Shen, R. Yu, Anal. Chim. Acta 651 (2009) 220–226.
[17] X. Bo, J. Bai, L. Wang, L. Guo, Talanta 81 (2010) 339–345.
[18] M.J. Song, S.W. Hwang, D. Whang, Talanta 80 (2010) 1648–1652.
[19] Z. Liu, B. Zhao, Y. Shi, C. Guo, H. Yang, Z. Li, Talanta 81 (2010) 1650–1654.
[20] Q. Chi, S. Dong, Anal. Chim. Acta 310 (1995) 429–436.
[21] X. Zeng, X. Liu, B. Kong, Y. Wang, W. Wei, Sens. Actuators, B 133 (2008) 381–386.
[22] S.R. Samms, S. Wasmus, R.F. Savinell, J. Electrochem. Soc. 143 (1996) 1225–1232.
[23] I. Yamaguchi, K. Osakada, T. Yamamoto, Macromolecules 30 (1997) 4288–4294.
[24] P. Staiti, M. Minutoli, S. Hocevar, J. Power Sources 90 (2000) 231–235.
[25] P. Mustarelli, E. Quartarone, S. Grandi, A. Carollo, A. Magistris, Adv. Mater. 20 (2008) 1339–1343.
[26] C.L. Donnici, D.H.M. Filho, L.L.C. Moreira, G.T. Reis, E.S. Cordeiro, I.M.F. Oliveira, S. Carvalho, E.P. Paniago, J. Braz. Chem. Soc. 9 (1998) 455–460.
[27] Y. Iwakura, K. Uno, Y. Imai, J. Polym. Sci. A Polym. Chem. 2 (1964) 2605–2615.
[28] K. Nakanishi, P.H. Solomon, Infrared Absorption Spectroscopy, Holden Day, San Francisco, 1997.
[29] T. Sugama, Mater. Lett. 58 (2004) 1307–1312.
[30] I. Losito, C. Malitesta, I. De Bari, C.D. Calvano, Thin Solid Films 473 (2005) 104–113.
[31] Z. Hu, J. Xu, Y. Tian, R. Peng, Y. Xian, Q. Ran, L. Jin, Carbon 48 (2010) 3729–3736.
[32] S.F. Wang, T. Chen, Z.L. Zhang, X.C. Shen, Z.X. Lu, D.W. Pang, K.Y. Wong, Langmuir 21 (2005) 9260–9266.
[33] Y. Ding, Y. Wang, B. Li, Y. Lei, Biosens. Bioelectron. 25 (2010) 2009–2015.
[34] S. Thiagarajan, S.M. Chen, Talanta 74 (2007) 212–222.
[35] X. Lu, J. Zhou, W. Lu, Q. Liu, J. Li, Biosens. Bioelectron. 23 (2008) 1236–1243.
[36] H.Y. Zhao, W. Zheng, Z.X. Meng, H.M. Zhou, X.X. Xu, Z. Li, Y.F. Zheng, Biosens. Bioelectron. 24 (2009) 2352–2357.
[37] S. Chen, R. Yuan, Y. Chai, L. Zhang, N. Wang, X. Li, Biosens. Bioelectron. 22 (2007) 1268–1274.
[38] F. Jia, C. Shan, F. Li, L. Niu, Biosens. Bioelectron. 24 (2008) 945–950.
[39] X. Xu, S. Jiang, Z. Hu, S. Liu, ACS Nano 4 (2010) 4292–4298.